

Crystal structure of synthetic $\text{Ca}_3\text{Mn}_2^{3+}\text{O}_2[\text{Si}_4\text{O}_{12}]^*$

Paul B. Moore and Takaharu Araki

Department of the Geophysical Sciences, The University of Chicago,
5734 South Ellis Avenue, Chicago, Illinois 60637, USA

Received: March 5, 1979

Abstract. The crystal structure of synthetic $\text{Ca}_3\text{Mn}_2^{3+}\text{O}_2[\text{Si}_4\text{O}_{12}]$ ($I2/c$, $a = 14.263(28)$, $b = 7.620(13)$, $c = 10.025(4)$ Å, $\beta = 93.27(5)^\circ$, $Z = 4$) has been determined and refined with anisotropic thermal parameters to $R = 0.038$ for 2342 independent F_o using $\text{MoK}\alpha_1$ radiation.

The structure is a new type and can be described consisting of three components which through corner- and edge-sharing link to form a polyhedral framework. One component is a ${}^1_{\infty}[\text{Si}_4\text{O}_{12}]$ chain parallel [010] which is isomorphic to a chain component $[\cdots\text{Mg}-\text{O}(3)-\text{Si}-\text{O}(3)-\text{Mg}-\text{O}(3)\cdots]$ parallel [100] or [010] in melilite, $\text{Ca}_2[\text{MgSi}_2\text{O}_7]$. The second component, also oriented parallel [010], is a ${}^1_{\infty}[\text{Ca}(2)\text{O}_6]$ edge-sharing chain made of distorted $\text{Ca}(2)\text{O}_8$ square antiprisms. The third component is a ${}^2_{\infty}[\text{Ca}(1)\text{Mn}_2^{3+}\text{O}_8]$ sheet oriented parallel to $\{100\}$. This sheet is made up of ${}^1_{\infty}[\text{Mn}^{3+}\text{O}_4]$ octahedral edge-sharing chains which run parallel to [001], alternately *trans*- $\text{Mn}(1)\text{O}_6$ and *cis*- $\text{Mn}(2)\text{O}_6$.

Polyhedral distance averages are ${}^{[6]}\text{Mn}(1)-\text{O}$ 2.027, ${}^{[6]}\text{Mn}(2)-\text{O}$ 2.046, ${}^{[8]}\text{Ca}(1)-\text{O}$ 2.663, ${}^{[8]}\text{Ca}(2)-\text{O}$ 2.539, $\text{Si}(1)-\text{O}$ 1.627 and $\text{Si}(2)-\text{O}$ 1.636 Å.

Introduction

We have been interested in the mineralogical crystal chemistry of Mn^{3+} which, according to its high spin d^4 arrangement in oxide environments, behaves much like high spin d^9 Cu^{2+} , and the two ions exhibit the consequent Jahn-Teller effect resulting in substantial distortion of the octahedrally coordinating oxyanions to form elongate or compressed square bipyramidal coordination polyhedra. Examples we have earlier studied include flinkite (Moore, 1967), pinakiolite (Moore and Araki, 1974), braunite

* Dedicated to Prof. W. Nowacki on occasion of his 70th birthday

(Moore and Araki, 1976) and two as yet unreported crystal structures of basic Ca–Mn³⁺-silicates, orientite and macfallite. Cations like Mn³⁺ and Cu²⁺ such as prevail in oxidative environments on Earth's crust are expected to behave differently in their geochemistry than more frequent Al³⁺ and Fe³⁺, and therefore are locally concentrated to form their own mineral species with unique structural chemistry, and limited solid solubility with the more prevalent octahedrally coordinated oxide cations such as Mg²⁺, Al³⁺, Fe³⁺ and Ti⁴⁺.

Therefore our interest was drawn to the phase CMS-XI recently communicated by Anastasiou and Langer (1977) who reported the composition $\text{Ca}_3\text{Mn}_2^{3+}(\text{Si}_2\text{O}_7)_2$. Although not yet reported as a mineral species, the aforementioned authors point out its stability only at relatively high pressure, at least greater than 13kB. It forms small prismatic intensely pleochroic crystals ranging from deep violet to light brown in color.

Experimental

Single crystals of CMS-XI coexisting with braunite and quartz were kindly supplied by Professor K. Langer of Universität Bonn. Considerable effort was required to secure a suitable crystal which was free from parasitic intergrowths or twinning. The crystal finally selected for study afforded experimental details in Table 1. Single crystal cell parameters were obtained from calibrated Buerger precession photographs using MoK α radiation.

Single crystal reflections on the Pailred diffractometer that were within the machine's blind regions were manually collected. The (0k0) reflections were estimated from precession films and were used only in the preliminary stages of structure analysis. Reflections of the regions (hkl) and (hkl), up to $k = 11$ were collected. For absorption correction, the crystal shape was approximated by 12 faces with 7 divisions for the Gaussian integral (Burnham, 1966). Extremes in transmission factors ranged from 0.587 to 0.721. "Unobserved" reflections with $I < 2\sigma(I)$ were set to $I = \sigma(I)$. Symmetry equivalent structure factors were then averaged giving 2341 independent data.

Three-dimensional Patterson synthesis, $P(uvw)$, allowed immediate interpretation of 6 heavy atom positions whose loci admitted 2 Mn, 2 Ca and 2 Si independent positions. As input into β -general synthesis (Ramachandran and Srinivasan, 1970), all remaining positions were revealed which included the 7 independent oxygen atoms. In the least-squares refinement, scattering curves were used for Ca²⁺, Mn³⁺, Si⁴⁺ and O¹⁻ from Ibers and Hamilton (1974). Convergence was reached at $R = 0.038$ and $R_w = 0.037$ where,

$$R = \frac{\sum ||F_o| - |F_c||}{\sum |F_o|} \text{ and } R_w = \left[\frac{\sum_w (|F_o| - |F_c|)^2}{\sum_w F_o^2} \right]^{1/2}$$

Table 1. Experimental details for CMS-XI ($\text{Ca}_3\text{Mn}_2\text{O}_2[\text{Si}_4\text{O}_{12}]$)

(A) Crystal cell data

a , Å	14.263(28)
b , Å	7.620(13)
c , Å	10.025(4)
β , deg	93.27(5)
Space group	$I2/c$
Z	4
Formula	$\text{Ca}_3\text{Mn}_2^3+\text{O}_2[\text{Si}_4\text{O}_{12}]$
ρ (calcd), g cm^{-3}	3.458
μ , cm^{-1}	42.67

(B) Intensity measurements

Crystal size, mm	0.15 ($\parallel a$), 0.11 ($\parallel b$), 0.09 ($\parallel c$)
Diffractometer	Pailred semi-automatic
Crystal orientation	b -axis rotation
Max $(\sin \theta)/\lambda$	0.75
Scan speed, deg per min	0.5
Base scan width, deg	2.8 (0-level) to 6.00 (higher levels)
Background counts	Stationary, 20 s at beginning and end of scan
Radiation	$\text{MoK}\alpha_1$ (λ 0.7093 Å)
Independent F_o	2341

(C) Refinement of the structure

R	0.038
R_w	0.037
Scale factor	1.569(3)
Coefficient of extinction	$2.1(5) \times 10^{-7}$

Table 2. The final positional parameters (standard deviations) for CMS-XI ($\text{Ca}_3\text{Mn}_2\text{O}_2[\text{Si}_4\text{O}_{12}]$)

Atom	x	y	z
Mn(1)	0	0	0
Mn(2)	0	0.78757(5)	$\frac{1}{4}$
Ca(1)	0	0.33998(8)	$\frac{1}{4}$
Ca(2)	0.19855(3)	0.03078(5)	0.23912(4)
Si(1)	0.32307(4)	0.21004(7)	0.98037(6)
Si(2)	0.37343(4)	0.16181(7)	0.52021(6)
O(1)	0.33375(12)	0.00688(20)	0.92714(16)
O(2)	0.27879(12)	0.22938(20)	0.59499(16)
O(3)	0.31786(12)	0.21005(19)	0.13822(16)
O(4)	0.44706(12)	0.09704(19)	0.63703(16)
O(5)	0.10262(12)	0.16276(18)	0.58584(17)
O(6)	0.08675(12)	0.20621(19)	0.08829(16)
O(7)	0.06569(12)	0.03690(20)	0.84803(17)

Table 3. CMS-XI ($\text{Ca}_3\text{Mn}_2\text{O}_2[\text{Si}_4\text{O}_{12}]$) anisotropic thermal parameters ($\times 10^5$)^a

Atom	β_{11}	β_{22}	β_{33}	β_{12}	β_{13}	β_{23}
Mn(1)	64(2)	215(5)	84(3)	5(3)	11(2)	13(3)
Mn(2)	76(2)	233(5)	109(4)	0	-13(2)	0
Ca(1)	184(3)	391(8)	171(5)	0	59(3)	0
Ca(2)	96(2)	315(5)	162(3)	-30(2)	20(2)	-28(3)
Si(1)	71(2)	206(7)	101(5)	0(3)	-0(3)	-0(4)
Si(2)	69(2)	226(7)	112(5)	-2(3)	7(3)	6(4)
O(1)	138(7)	262(17)	149(13)	30(10)	-34(8)	-12(12)
O(2)	75(6)	463(21)	151(13)	27(10)	0(7)	18(13)
O(3)	138(7)	329(19)	121(12)	-15(10)	24(8)	-3(13)
O(4)	116(7)	241(18)	159(13)	-5(9)	-39(8)	5(12)
O(5)	92(7)	278(19)	186(13)	-35(9)	27(8)	-3(13)
O(6)	115(7)	278(18)	141(12)	-17(9)	5(7)	12(13)
O(7)	101(7)	428(20)	135(12)	51(9)	34(8)	81(13)

^a Coefficients in the expression $\exp -[\beta_{11}h^2 + \beta_{22}k^2 + \beta_{33}l^2 + 2\beta_{12}hk + 2\beta_{13}hl + 2\beta_{23}kl]$. Estimated standard errors refer to the last digit except for those coefficients related by symmetry.

The final cycle minimized $\sum_w ||F_o| - |F_c||^2$ where $w = \sigma^{-2}(F)$. The ratio of number of independent F 's to number of varied parameters is 22:1 and included the anisotropic thermal motions.

The refined atomic coordinate parameters appear in Table 2. Table 3 presents anisotropic thermal vibration parameters, Table 4 the ellipsoids of vibration. Table 5 polyhedral interatomic distances and Table 6 a calculated powder pattern (FeK α radiation) from the structure data and equivalent isotropic thermal vibration parameters. A list of observed and calculated structure factors has been deposited at the publisher.

Results and discussion

Structure geometry and topology

At first we suspected CMS-XI to be crystallochemically identical with $\text{Ca}_3\text{Mn}_6^{3+}[\text{Si}_2\text{O}_7]_2$, the formula proposed by Anastasiou and Langer (1977), and that it may be based on sorosilicate doublets or possibly related to the braunite, $(\text{Mn,Ca})^{2+}\text{Mn}_2^{3+}\text{O}_8[\text{SiO}_4]$, structure through extensive exploitation of (SiO_4) tetrahedra on a design based on an anion deficient fluorite derivative structure (Moore and Araki, 1976). The structure analysis, however, revealed a surprising feature: that CMS-XI is a chain silicate, thus properly an oxy-silicate, $\text{Ca}_3\text{Mn}_2^{3+}\text{O}_2[\text{Si}_4\text{O}_{12}]$. The silicate chain component, however, is not related to the pyroxene-type chains but closely identifies with

Table 4. CMS-XI ($\text{Ca}_3\text{Mn}_2\text{O}_2[\text{Si}_4\text{O}_{12}]$) parameters for the ellipsoids of vibration^a

Atom	<i>i</i>	μ_i	θ_{ia}	θ_{ib}	θ_{ic}	B_{eq} \AA^2	Atom	<i>i</i>	μ_i	θ_{ia}	θ_{ib}	θ_{ic}	B_{eq} \AA^2
O(1)	1	0.081(4)	69(6)	99(31)	26(18)	0.78(2)	Mn(1)	1	0.064(1)	101(3)	101(3)	13(3)	0.45(1)
	2	0.086(3)	82(12)	165(18)	103(30)			2	0.079(1)	54(9)	144(10)	94(4)	
	3	0.126(3)	157(3)	102(4)	68(4)			3	0.083(1)	38(9)	56(9)	77(3)	
O(2)	1	0.083(4)	43(26)	103(5)	53(24)	0.76(2)	Mn(2)	1	0.071(1)	67(2)	90	26(3)	0.53(1)
	2	0.090(4)	49(23)	94(7)	142(27)			2	0.083(1)	90	180	90	
	3	0.118(3)	78(5)	14(5)	86(5)			3	0.092(1)	157(2)	90	64(3)	
O(3)	1	0.077(4)	100(4)	91(8)	7(4)	0.79(2)	Ca(1)	1	0.086(1)	109(1)	90	16(1)	1.02(1)
	2	0.098(3)	100(6)	170(7)	92(8)			2	0.107(1)	90	180	90	
	3	0.120(3)	14(6)	100(6)	84(4)			3	0.141(1)	19(1)	90	74(1)	
O(4)	1	0.079(4)	62(5)	94(33)	32(7)	0.72(2)	Ca(2)	1	0.087(1)	89(12)	57(10)	34(13)	0.72(1)
	2	0.084(3)	94(16)	176(30)	92(28)			2	0.089(1)	43(3)	56(10)	116(16)	
	3	0.119(3)	151(3)	87(4)	58(4)			3	0.108(1)	47(2)	128(2)	70(2)	
O(5)	1	0.081(1)	130(7)	136(8)	72(11)	0.71(2)	Si(1)	1	0.071(2)	97(5)	107(9)	18(9)	0.49(1)
	2	0.094(3)	75(11)	122(12)	145(12)			2	0.078(1)	103(8)	157(9)	108(9)	
	3	0.107(3)	43(8)	116(9)	61(11)			3	0.086(1)	15(7)	105(7)	91(5)	
O(6)	1	0.083(4)	94(8)	114(22)	24(22)	0.72(2)	Si(2)	1	0.075(2)	98(8)	104(9)	14(9)	0.51(1)
	2	0.090(3)	103(8)	151(22)	114(22)			2	0.082(1)	104(25)	159(21)	104(9)	
	3	0.110(3)	166(10)	76(7)	85(7)			3	0.084(2)	16(21)	106(24)	89(10)	
O(7)	1	0.073(4)	103(8)	108(5)	21(3)	0.78(2)							
	2	0.092(4)	147(5)	57(6)	88(8)								
	3	0.126(3)	60(4)	39(4)	69(3)								

^a *i* = *i*th principal axis; μ_i = rms amplitude; θ_{ia} , θ_{ib} , θ_{ic} = angles between the *i*th principal axis and the cell axes *a*, *b* and *c*. The equivalent isotropic thermal vibration parameters are also stated

Table 5. Polyhedral interatomic distances and angles in CMS-XI ($\text{Ca}_3\text{Mn}_2\text{O}_2[\text{Si}_4\text{O}_{12}]$)

Mn(1)		Si(1)		Ca(1)	
Mn(1)–O(7)	(×2)	Si(1)–O(3)	1.588(2)	Ca(1)–O(6)	2.330(2) Å (×2)
–O(5) ⁽²⁾	(×2)	–O(5) ⁽⁵⁾	1.607(2)	–O(4) ⁽⁴⁾	2.365(3) (×2)
–O(6)	(×2)	–O(1)	1.647(3)	–O(3) ⁽⁵⁾	2.796(5) (×2)
mean	2.027 Å	O(2) ⁽⁵⁾	1.664(3)	–O(7) ⁽¹⁾	3.160(5) (×2)
		mean	1.627	mean	2.663
O(5) ⁽²⁾ –O(7) ⁽¹⁾	(×2)	O(2) ⁽⁵⁾ –O(5) ⁽⁵⁾	2.560(5)		Ca(2)
O(6)–O(7)	86.9(1)	O(1)–O(2) ⁽⁵⁾	2.574(3)	Ca(2)–O(7) ⁽²⁾	2.299(4)
O(5) ⁽²⁾ –O(7) ⁽¹⁾	85.5(1)	O(1)–O(3)	2.642(3)	–O(3) ⁽⁵⁾	2.345(3)
O(5) ⁽²⁾ –O(7) ⁽¹⁾	83.7(1)	O(1)–O(5) ⁽⁵⁾	2.681(5)	–O(3)	2.446(3)
O(5) ⁽²⁾ –O(7) ⁽¹⁾	93.1(1)	O(2) ⁽⁵⁾ –O(3)	2.685(3)	–O(5) ⁽²⁾	2.484(3)
O(6)–O(7) ⁽¹⁾	94.5(1)	O(3)–O(5) ⁽⁵⁾	2.750(3)	–O(6)	2.518(3)
O(5) ⁽²⁾ –O(6)	96.3(1)	mean	2.649	–O(1) ⁽²⁾	2.634(3)
mean	90.0			–O(2) ⁽²⁾	2.742(3)
				–O(2) ⁽⁷⁾	2.843(4)
				mean	2.539
Mn(2)		Si(2)			
Mn(2)–O(7) ⁽¹⁾	(×2)	Si(2)–O(4)	1.606(2)		
–O(4) ⁽⁴⁾	(×2)	–O(6) ⁽⁵⁾	1.609(2)		
–O(5) ⁽¹⁾	(×2)	–O(2)	1.663(3)		
mean	2.046	–O(1) ⁽²⁾	1.668(2)		
		mean	1.636		
O(7) ⁽¹⁾ –O(7) ⁽²⁾	89.2(2)	O(1) ⁽²⁾ –O(6) ⁽⁵⁾	2.565(4)		
O(4) ⁽⁴⁾ –O(4) ⁽⁷⁾	84.8(1)	O(1) ⁽²⁾ –O(2)	2.615(3)		
O(5) ⁽²⁾ –O(7) ⁽¹⁾	80.0(1)	O(2)–O(4)	2.615(5)		
O(4) ⁽⁴⁾ –O(7) ⁽¹⁾	93.5(1)	O(1) ⁽²⁾ –O(4)	2.698(3)		
O(5) ⁽¹⁾ –O(7) ⁽¹⁾	86.5(1)	O(4)–O(6) ⁽⁵⁾	2.731(3)		
O(4) ⁽⁴⁾ –O(5) ⁽²⁾	87.0(1)	O(2)–O(6) ⁽⁵⁾	2.774(4)		
O(4) ⁽⁴⁾ –O(5) ⁽¹⁾	107.2(1)	mean	2.666		
mean	90.2				

^a The angles refer to the O–Mn (or Si)–O' angles associated with the listed edges. ^b Shared edge between two Mn^{3+} cations.

^c Shared edge between Mn^{3+} and Ca^{2+} cations. Based on the list in Table 2, the equipoins are designated as superscripts: (1) $-x, -y, -z$; (2) $x, -y, \frac{1}{2} + z$; (3) $-x, y, \frac{1}{2} + z$; (4) $\frac{1}{2} + x, \frac{1}{2} + y, \frac{1}{2} + z$; (5) $\frac{1}{2} - x, \frac{1}{2} - y, \frac{1}{2} - z$; (6) $\frac{1}{2} + x, \frac{1}{2} - y, \frac{1}{2} - z$; (7) $\frac{1}{2} - x, \frac{1}{2} + y, -z$.

Table 6. Calculated powder pattern for CMS-XI^a ($\text{Ca}_3\text{Mn}_2\text{O}_2[\text{Si}_4\text{O}_{12}]$)

	<i>I</i> (calc)	<i>I</i> (obs)	<i>d</i> (calc)	<i>d</i> (obs)	<i>h</i>	<i>k</i>	<i>l</i>
	14	—	7.120	—	2	0	0
	29	—	6.718	—	1	1	0
	12	—	4.697	—	$\bar{2}$	1	1
	11	—	3.438	—	1	2	1
	100	100	3.215	3.208	$\bar{3}$	1	2
	23	—	3.117	—	$\bar{4}$	1	1
	69	30	3.067	3.063	3	1	2
	13	—	3.056	—	0	1	3
	34	—	2.982	—	$\bar{4}$	0	2
	19	—	2.826	—	4	0	2
	58	70	2.824	2.821	$\bar{2}$	2	2
	31	—	2.821	—	3	2	1
	60	40	2.755	2.754	2	2	2
	15	—	2.502	—	0	0	4
	18	—	2.500	—	1	3	0
	12	—	2.490	—	$\bar{1}$	2	3
	16	—	2.373	—	6	0	0
	60	30	2.270	2.267	4	2	2
	11	—	2.228	—	1	3	2
	15	—	1.896	—	5	3	0
	18	—	1.876	—	$\bar{5}$	1	4

^a Based on $\text{FeK}\alpha$ radiation, atomic coordinate parameters in Table 2, equivalent isotropic thermal parameters in Table 4. The observed data are from Anastasiou and Langer (1977).

a chain component in the melilite, $\text{Ca}_2[\text{MgSi}_2\text{O}_7]$ structure. Since melilite can be conceived as a sheet structure with T_3O_7 stoichiometry, a variety of chain components can be extracted, the one of interest here being a crankshaft chain component parallel to $[100]$ or $[010]$ in melilite consisting of links $(\cdots \text{Mg}-\text{O}(3)-\text{Si}-\text{O}(3)-\text{Mg}-\text{O}(3)\cdots)$. Excepting the larger MgO_4 tetrahedron, the chain components are well-superimposed in both structures, with a_1 (melilite) = 7.79 Å (Smith, 1953) to be compared with $b = 7.62$ Å in CMS-XI. The T–O–T angles are 118.4° in melilite $[\text{Mg}-\text{O}(3)-\text{Si}]$, and 125.3° $[\text{Si}(1)-\text{O}(1)-\text{Si}(2)]$ and 126.3° $[\text{Si}(1)-\text{O}(2)-\text{Si}(2)]$ in CMS-XI, the tetrahedral orientations in both structures being approximately the same. One chain component in CMS-XI is shown in Fig. 1.

But the CMS-XI structure is rather complex and best considered as consisting of three components which link through shared oxygens to form a complicated framework. Two components consist of the $\frac{1}{\infty}[\text{Si}_4\text{O}_{12}]$ and $\frac{1}{\infty}[\text{Ca}(2)\text{O}_6]$ chains which run parallel to $[010]$. The $\text{Ca}(2)\text{O}_6$ polyhedron is a distorted square antiprism which shares $\text{O}(3)-\text{O}(3)'$ and $\text{O}(2)-\text{O}(2)'$ edges across inversion centers (Fig. 2). The third component is a sheet $\frac{2}{\infty}[\text{Ca}(1)\text{Mn}_2^3+\text{O}_8]$ oriented parallel to $\{100\}$ and possessing two-sided plane

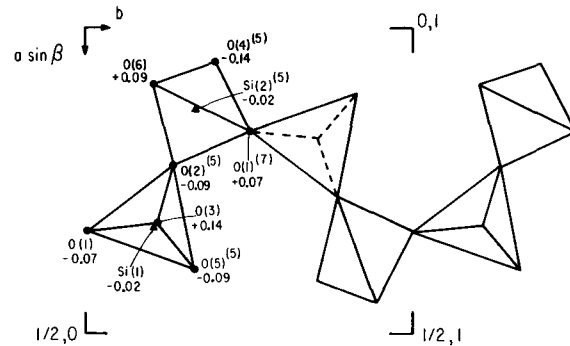


Fig. 1. $\text{Ca}_3\text{Mn}_2\text{O}_2[\text{Si}_4\text{O}_{12}]$. The $\frac{1}{\infty}[\text{Si}_4\text{O}_{12}]$ chain component down the z -axis. Heights are given as fractional coordinates in z . Atoms are labeled according to Table 5

group $p2/c$ (Fig. 3). In this sheet, O(3) associated with Ca(1) has been omitted, yielding a distorted octahedral sheet of ideal stoichiometry M_3O_8 and topologically isomorphic to sheet D, the isomer of the octahedral sheet in chloritoid and down $[111]$ in spinel (Moore, 1972). The sheet component is based on zig-zag $\frac{1}{\infty}[\text{Mn}^{3+}\text{O}_4]$ octahedral edge-sharing chains which run parallel to $[001]$, alternately *trans*-Mn(1) O_6 and *cis*-Mn(2) O_6 , the shared edges being O(5)–O(7). It is distinct from the linear $\frac{1}{\infty}[\text{trans-Mn}^{3+}\text{O}_4]$ chain in bermanite (Kampf and Moore, 1976) and the $\frac{1}{\infty}[\text{cis-Al}^{3+}\text{O}_4]$ chain found in foggite and Ca-Tschermak's pyroxene (Moore, Kampf and Araki, 1975). The sheet is bridged above the O(5)–O(6)–O(7) triangular "tetrahedral hole" by edge-sharing Ca(2), and by O(4) and O(6) corner-links to Si(2), and O(5) to Si(1), completing the structure.

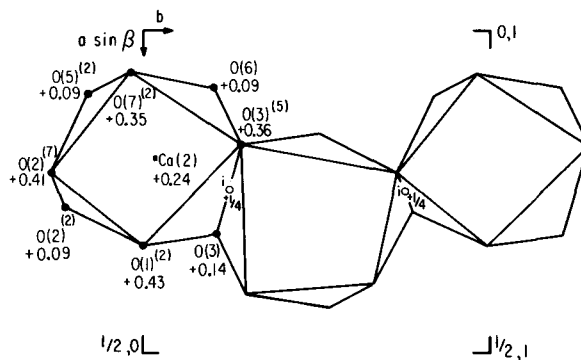


Fig. 2. $\text{Ca}_3\text{Mn}_2\text{O}_2[\text{Si}_4\text{O}_{12}]$. The $\frac{1}{\infty}[\text{Ca}(2)\text{O}_6]$ edge-sharing chain of distorted square antiprisms which run parallel to the b -direction. Heights are given as fractional coordinates in z . Atoms are labelled according to Table 5. Note the loci of inversion centers at the midpoints of shared edges

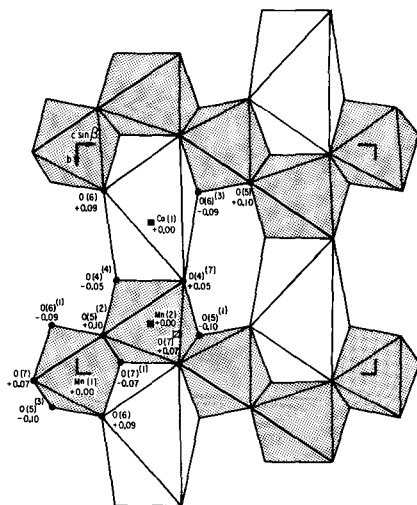


Fig. 3. $\text{Ca}_3\text{Mn}_2\text{O}_2[\text{Si}_4\text{O}_{12}]$. The $\infty[\text{Ca}(1)\text{Mn}_2^3+\text{O}_8]$ sheet oriented parallel to $\{100\}$. Atoms are labelled according to Table 5. The O(3) atoms which also coordinate to Ca(1) are omitted and are situated roughly above O(4)⁽⁴⁾ and O(4)⁽⁷⁾. The $\infty[\text{Mn}^3+\text{O}_4]$ octahedral chains are stippled

Polyhedral interatomic distances

Bond distances and angles are presented in Table 6. As expected, the Mn^3+O_6 octahedra are substantially distorted owing to d^4 high-spin Jahn-Teller distortion of Mn^3+ in an oxide environment. Although Mn(2) possesses four short and two long bonds defining an elongate square bipyramid, Mn(1) is more complicated since elongate and square planar vertices cannot be easily ascribed, unlike orthopinakiole and related structures (Takéuchi et al., 1978). This may result from bond length-bond strength effects, given in Table 7 adopting to procedures of Baur (1970) where Mn^3+-O was assigned a uniform bond strength of $s = 3/6$ distinct from elongate bond strength of $s = 4/12$ and square planar bond strength of $s = 7/12$, ascribed by Kampf and Moore (1976) in the analysis of bermanite, where elongate square bipyramidal aspect is more pronounced. O(7) which is coordinated by Mn(1) + Mn(2) + Ca(1) + Ca(2) is seriously undersaturated by cations and three of the bonds, those associated with Mn(1), Mn(2) and Ca(2), are substantially shorter than average. The $\text{Ca}(1)-\text{O}(7) = 3.160 \text{ \AA}$ bond distance could be considered beyond the first coordination sphere but this long distance may also be a result of cation-cation repulsion by the three Mn^3+ cations on the opposite side, and the Ca(1) atom. Such long distances for Ca-O bonds are frequently encountered in structures of complex oxides containing Ca^{2+} and the definition of true coordination number is not clear.

Table 7. CMS-XI ($\text{Ca}_3\text{Mn}_2\text{O}_2[\text{Si}_4\text{O}_{12}]$). Relations in bond strength-bond length^a

Anions	Coordinating cations						Bond length deviations						
	Si(1)	Si(2)	Mn(1)	Mn(2)	Ca(1)	Ca(2)	Δp_0	Si(1)	Si(2)	Mn(1)	Mn(2)	Ca(1)	Ca(2)
O(1)	1	1	-	-	-	1	+0.25	+0.020	+0.032	-	-	-	+0.095
O(2)	1	1	-	-	-	2	+0.50	+0.037	+0.027	-	-	-	+0.203
O(3)	1	-	-	-	1	2	-0.25	-0.039	-	-	-	+0.133	-0.093
O(4)	-	1	-	1	1	-	-0.25	-	-0.030	-	-0.081	-0.298	-
O(5)	1	-	1	1	-	1	+0.25	-0.020	±	+0.041	+0.249	-	-0.055
O(6)	-	1	1	-	1	1	+0.00	-	-0.027	+0.131	-	-0.333	-0.021
O(7)	-	-	1	1	1	1	-0.50	-	-	-0.172	-0.168	+0.497	-0.240

^a Δp_0 is the deviation of the bond strength sum from neutrality ($p_0 = 2.000$). A bond length deviation is the polyhedral average subtracted from the individual bond distance.

Of the remaining coordinating anions, O(1), O(2) and O(4) show bond length-bond strength deviations which are in accord with longer (shorter) bonds associated with oversaturated (undersaturated) anions. As with O(7); O(3), O(5) and O(6) display contradictions but these are compensated by cation-oxygen distances which conform with overall oversaturation or undersaturation of anions by cations.

Acknowledgments. We thank Professor Dr. K. Langer of Universität Bonn for the single crystals of CMS-XI and for his valuable discussion on phases in the system $\text{CaO}-\text{Al}_2\text{O}_3-(\text{MnO}-\text{MnO}_2)-\text{SiO}_2-\text{H}_2\text{O}$. This work was supported by the National Science Foundation grant EAR-75-19483 (Geochemistry) awarded to P.B.M.

References

- Anastasiou, P., Langer, K.: Synthesis and physical properties of piemontite $\text{Ca}_2\text{Al}_3\text{-pMn}_p^{3+}$ ($\text{Si}_2\text{O}_7/\text{SiO}_4/\text{O}/\text{OH}$). *Contrib. Mineral. Petrol.* **60**, 225–245 (1977)
- Baur, W. H.: Bond length variation and distorted coordination polyhedra in inorganic crystals. *Trans. Amer. Crystallogr. Assoc.* **6**, 129–155 (1970)
- Ibers, J. A., Hamilton, W. C., (Eds.): *International tables for X-ray crystallography*, vol. IV, p. 149. Birmingham: Kynoch Press 1974
- Kampf, A. R., Moore, P. B.: The crystal structure of bermanite, a hydrated manganese phosphate mineral. *Amer. Mineral.* **61**, 1241–1248 (1976)
- Moore, P. B.: Aluminum, 13-A. In: *Handbook of geochemistry*, vol. II/3 (K. H. Wedepohl, ed.), p. 13-A-5. Berlin, Heidelberg, New York: Springer 1972
- Moore, P. B.: The crystal structures of flinkite and retzian. *Amer. Mineral.* **52**, 1603–1613 (1967)
- Moore, P. B., Araki, T.: Pinakiolite, warwickite and wightmanite: crystal chemistry of complex 3 Å wallpaper structures. *Amer. Mineral.* **59**, 985–1004 (1974)
- Moore, P. B., Araki, T.: Braunitz: its structure and relationship to bixbyite, and some insights on the genealogy of fluorite derivative structures. *Amer. Mineral.* **61**, 1226–1240 (1976)
- Moore, P. B., Kampf, A. R., Araki, T.: Foggite: its atomic arrangement and relationship to calcium Tschermak's pyroxene. *Amer. Mineral.* **60**, 965–971 (1975)
- Smith, J. V.: Reexamination of the crystal structure of melilite. *Amer. Mineral.* **38**, 643–661 (1953)
- Ramachandran, G. N., Srinivasan, R.: *Fourier methods in crystallography*, 96–119. New York: Wiley-Interscience 1970
- Takéuchi, Y., Haga, N., Kato, T., Miura, Y.: Orthopinakiolite: its crystal structure and relationship to pinakiolite. *Canad. Mineral.* **16**, 475–485 (1978)